

## PALAEOMAGNETIC INVESTIGATIONS IN HIGHLY METAMORPHOSED ROCKS: EASTERN ALPS (AUSTRIA AND HUNGARY)

Herman J. MAURITSCH\*, Emő MÁRTON\*\* and Alfred PAHR\*\*\*

A palaeomagnetic study was carried out in a tectonically complex area, mainly on highly metamorphosed rocks. Nine sites in the Penninic unit, one site in the Palaeozoic of Graz and one in the Wechsel unit, yielded characteristic remanent magnetizations (ChRM). The ChRMs were further tested in order to estimate the age of acquisition and magnitude of a possible bias of the observed directions due to metamorphism. It is concluded that the studied metamorphic rocks must have been fully overprinted during the last phase of metamorphism in the area and the oriented magnetic fabric could only have had but a minor influence on the direction of remanence.

The directions of the characteristic remanences — both before and after tectonic correction — depart significantly from that of the Earth's present magnetic field observed at the sampling area. The scatter is too high to define palaeomagnetic directions for any of the tectonic units. Tendencies in the declination rotations, however, may be recognized and interpreted as tectonic rotations. Apart from the highest level, the Penninic is clockwise, the top of the Penninic — together with the cover of Karpathian and Badenian age — is counterclockwise rotated. The sense of rotation is uncertain for the Wechsel unit because of the shallowness of the observed inclination. The observed rotations must be mainly due to mid-Miocene tectonic movements, postdating both the deposition of the Karpathian sediments and the last phase of metamorphism at 20 Ma.

**Keywords:** Palaeomagnetism, metamorphic rocks, Eastern Alps, magnetic fabric, ChRM, tectonic rotation

### 1. Introduction

The investigated area belongs to the eastern part of the Eastern Alps, where the Penninic crops out (*Fig. 1*) such as the windows of Möltern, Bernstein and Rechnitz [SCHMIDT 1951]. They are parts of a chain of windows exposing the lowermost tectonic unit of the Alps between Genoa, Italy, and Kőszeg, Hungary.

The Penninic unit is characterized by a particular lithology and metamorphism, showing all the elements of an ocean floor development, such as calcareous phyllites, limestone shales, quartzites, greenschists, serpentinites, and metagabbros. The sequence is dated mid-Cretaceous by sponge spiculae in limestone members [SCHÖNLAUB 1973].

The geological environment of the windows of Möltern and Bernstein is dominated by overthrust crystalline rocks of the Lower East-Alpine Wechsel

\* Institute of Geophysics, Mining University, Leoben, Franz Josef Street 18, A-8700, Leoben, Austria

\*\* Eötvös Loránd Geophysical Institute, Budapest, POB 35, H-1440, Hungary

\*\*\* Geologische Bundesanstalt, 1031 Vienna, Rasumofskygasse 23, Austria

Manuscript received (revised version): 13 October, 1990

unit. The Rechnitz and Eisenberg windows are surrounded by Tertiary sediments of Karpathian through Pannonian age.

The Tertiary cover conceals the tectonic situation in the southern part of the investigated area. Nevertheless, we know from other observations that it is not simple. For instance, the greenschist of Hannersdorf (Fig. 1, site 13) and its surroundings cannot belong to the Penninic in spite of the similar lithology and the present geographic position. The arguments are stratigraphical — as the age of the Hannersdorf dolomite is Devonian in contrast to the Cretaceous age of the Penninic — and geochemical, as the Penninic is derived from the ocean floor whereas the greenschist of Hannersdorf is a metamorphosed intra-plate basalt [GRATZER 1985]. Concerning the metamorphism in this area, three main phases have been recognized [LELKES-FELVÁRI 1982, KOLLER 1985]:

a) oceanic metamorphism at high temperatures ( $500\text{--}750^\circ\text{C}$ );

b) metamorphism during subduction at high pressure ( $6\text{--}8 \times 10^8\text{ Pa}$ ) and low temperature ( $300\text{--}370^\circ\text{C}$ ); these conditions require subsidence of the sediments of the Penninic ocean to a depth of about 15–25 km; the metamorphism is dated at  $65 \pm 6\text{ Ma}$  by the K/Ar method.

c) Regional metamorphism at pressures less than  $3 \times 10^8\text{ Pa}$  and temperatures of  $390\text{--}430^\circ\text{C}$  (greenschist facies); this event is dated at 19–22 Ma by the K/Ar method. It seems that the temperature of the metamorphism increases from north to south.

Based on *b*-axis orientation and the degree of complexity of the metamorphic texture, the Penninic may be subdivided into two nappe systems, both emplaced after the last phase of metamorphism. In the lower unit the *b*-axes are usually N–S oriented, in the upper unit they lie close to the E–W direction [PAHR 1980]. Members of the lower unit may be recognized as such by observing crenulations in addition to the dominant schistosity, since crenulation is totally absent in the upper nappe system.

## 2. Sampling and analysis of magnetic remanence

Six to twenty-six cores were drilled at twenty four sites in greenschists, calcareous phyllites, quartz phyllites, serpentinites belonging to the Penninic unit (Fig. 1, sites 1–12, 14–18, 24), in amphibolites and albite–chlorite–quartz schists of the Wechsel unit (Fig. 1, sites 21–23), greenschist belonging to the Palaeozoic of Graz (Fig. 1, site 13,) and in Tertiary sediments (Fig. 1, sites 19 and 25); 332 samples in all. The cores were oriented by a magnetic compass. Orientation of schistosity planes and fold-axes were measured in the field as precisely as possible. These observations were meant to serve a double purpose: firstly, to facilitate full tectonic correction of the palaeomagnetic directions; secondly, to decide whether the site belonged to the lower or the upper nappe system. The serpentinite of Bernstein (Fig. 1, site 24) was the only site at which tectonic elements could not be measured.

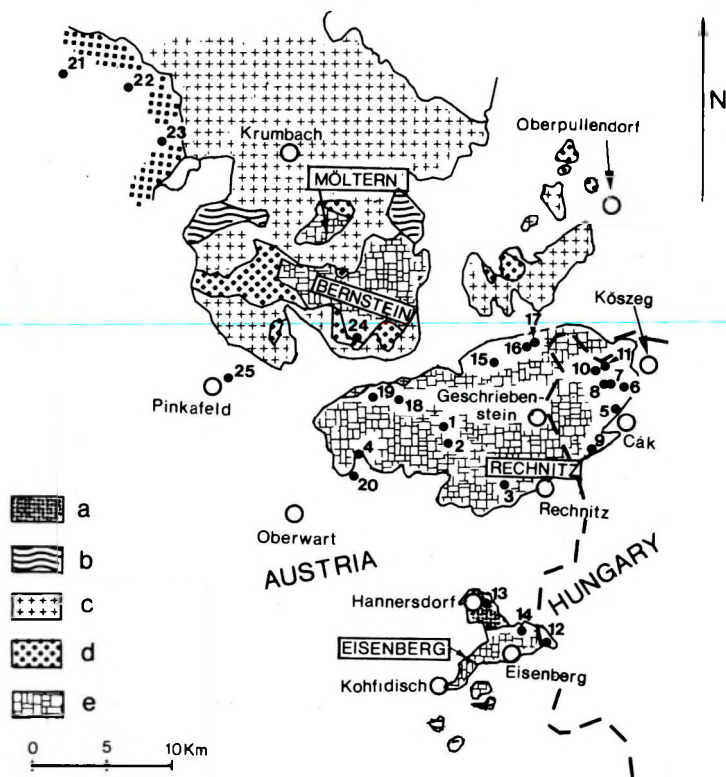


Fig. 1. Geological sketch map of the eastern part of the Eastern Alps with palaeomagnetic sampling sites. Key to geology: a) Upper East-Alpine Palaeozoic, b) Middle East-Alpine Crystalline, c) Lower East-Alpine Grogneiss unit, d) Lower East-Alpine Wechsel unit, e) Penninic. Sampling sites are in the Penninic of the Rechnitz window (sites 1-11, 18), of the Eisenberg window (sites 12 and 14) and of the Bernstein window (site 24), in the Palaeozoic of Graz (13), in the Wechsel unit (sites 21-23), in Karpathian (site 19) and Badenian (site 25) sediments covering the Grogneiss unit

1. ábra. Földtani vázlat a Keleti Alpok keleti részéről, a paleomágneses mintavételi helyekkel. Jelmagyarázat: a) Felső Keletalpi paleozoikum, b) Középső Keletalpi kristályos egység, c) Alsó Keletalpi Grogneiss egység, d) Alsó Keletalpi Wechsel egység, e) Penninikum. Mintavételi helyek a Penninikumon: a Rohonci ablakból (1-11 és 18), a Vashegyi ablakból (12 és 14) és a Bernstein ablakból (24); a grazi paleozoikumon (13), a Wechsel egységen (21-23), és a Grogneiss egység fedőjét képező kárpáti (19) és badeni (25) üledékeken

Рис. 1. Геологическая схема восточного окончания Восточных Альп с обозначением пунктов отбора проб на палеомагнитные определения  
 а) верхне-восточноальпийский палеозой, б) — средневосточноальпийские кристаллические комплексы, в) нижневосточноальпийские грубые гнейсы, д) нижневосточноальпийский Вехсельский покров, е) Пеннинский покров. Пункты отбора проб из Пеннинского покрова: по Кёсегско-Рехницскому окну (1-11 и 18), по Вашхельско-Айзенбергскому окну (12 и 14), по Бернштайнскому окну (24); из грацкого палеозоя (13); из Вехсельского покрова (21-23); из осадочного чехла единицы грубых гнейсов: по карпатским отложениям (19), по баденским отложениям (25)

The field cores were cut into 2–4 standard-size samples. From each core, sister specimens were subjected to stepwise demagnetization, both by AF and by the thermal method, independently in the palaeomagnetic laboratories in Budapest and at Gams. Full demagnetization was rarely achieved with AF (only at sites 24 and 25, see *Fig. 3*). Thermal demagnetization combined with AF or alone were more efficient (*Fig. 2* and *Fig. 4*). Where full coercivity or a blocking temperature spectrum was available, palaeomagnetic site mean directions were calculated combining first the characteristic remanences of sister specimens on sample, then on site level (sites 3, 10, 14, 18, 22, 25); samples with sister specimens of different directions (angular difference higher than 25°) were rejected (*Fig. 5*).

Unstable behaviour on cleaning often prevented complete demagnetization. Samples with dominant spurious components were disregarded. Moderate instability, however, was dealt with in the following way. After removing an obviously different and moderately resistant component, remanence directions measured at successive heating steps were averaged to enhance the signal (*Fig. 6*), provided that the susceptibility had not increased considerably.

The remanence directions thus obtained served as a basis for calculating site means (Table I. sites 4, 6, 8, 13, 24, 12<sub>1</sub>). At site 12 the component with the higher blocking temperature was further tested by repeating the demagnetization at the same temperature twice, first placing the specimen in the oven in one direction, then in the other, i.e. with *X* and *Z* in two opposite orientations; finally, the results of four cleaning steps — two at 450° C and two at 475° C — were averaged. This was done because of the moderate increase in susceptibility (20 per cent on average above 250–350° C, relative to the initial value).

*Table 1*<sup>1</sup> summarizes the ChRM directions before and after tilt (sites 19 and 25) or full tectonic correction — first for the *b*-axis tilt, then for the schistosity position, the latter being assumed to be parallel to the bedding for most sites.

<sup>1</sup> All samples bear the code of HA (for Hungary and Austria)

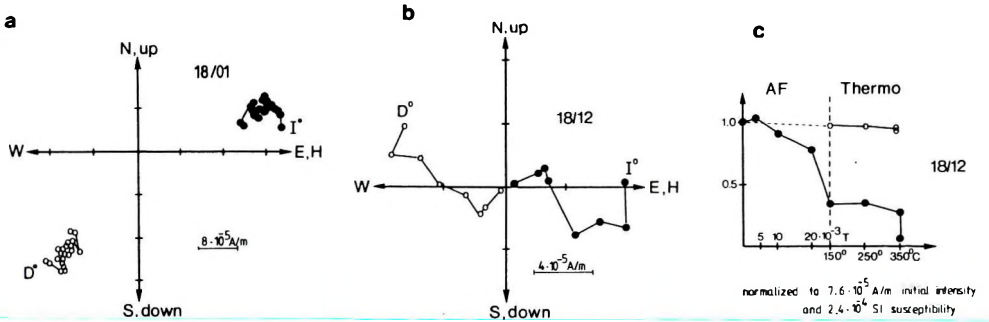


Fig. 2. Comparison of the behaviour of the NRM on AF (a) and on the combined AF and thermal (b, c) demagnetization. Rechnitz window, Penninic at Steinwandriegel (site 18): a) and b) are orthogonal plots (demagnetization steps in a): NRM to  $1 \times 10^{-2} T$ , in b) as in c)), c) is a normalized intensity (dots) and susceptibility (circles) diagram

2. ábra. Az NRM viselkedésének összehasonlítása váltóáramú (a) és kombinált váltóáramú- és termo- (b és c) lemágnesezésre. Rohonci ablak, Steinwandriegel, Penninikum (18. mintavételi hely): a) és b) ortogonális vetület (lemágnesezési lépések a)-ban: NRM-től  $1 \times 10^{-2} T$ -ig, b) és c) azonos, c) normalizált intenzitás (teli körök) és szuszceptibilitás (üres körök) diagram

Рис. 2. Сопоставление поведения NRM при чистке переменным током (a), а также комбинацией переменного тока с нагреванием (b и c). Рехницское окно, Штайнвандригель, Пеннинский покров (пункт пробоотбора 18): а) и б) прямоугольная проекция; ступени чистки в а) от NRM до  $1 \cdot 10^{-2} T$ ; б) и c) одинаковы; c) диаграмма нормированной интенсивности (залитые кружки) и восприимчивости (полые кружки)

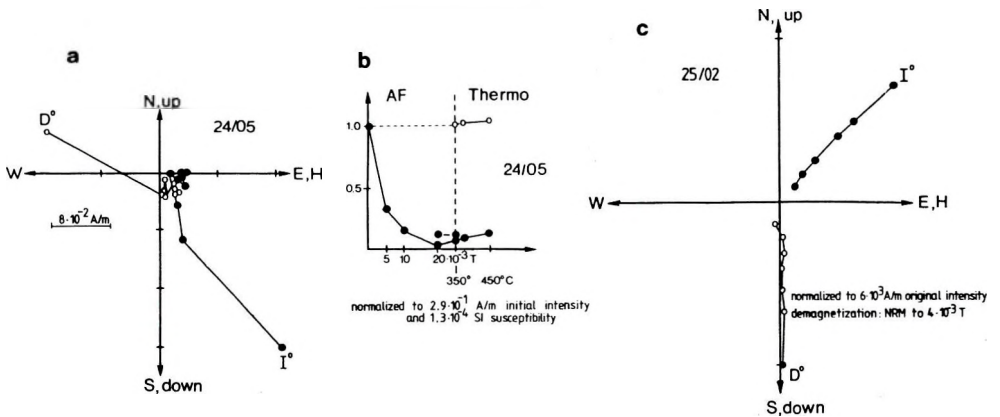


Fig. 3. Fast reduction of the NRM intensity on AF demagnetization. a) and b) Bernstein window, serpentinite (site 24) c) Badenian sediment (site 25). For explanation, see Fig. 2. (demagnetization steps: NRM to  $4 \times 10^{-3} T$ )

3. ábra. Az NRM gyors csökkenése váltóáramú lemágnesezésre. a) és b) Bernstein ablak, szerpentinít (24), c) bádeni üledék (25).

Jelmagyarázatot lásd a 2. ábrán (lemágnesezési lépések: NRM-től  $4 \times 10^{-3} T$ -ig)

Рис. 3. Быстрое убывание NRM при чистке переменным током. а) и б) Бернштайнское окно, серпентиниты (24), c) баденские отложения (25). Условные обозначения см. на рис. 2. Ступени чистки — от NRM до  $4 \cdot 10^{-3} T$

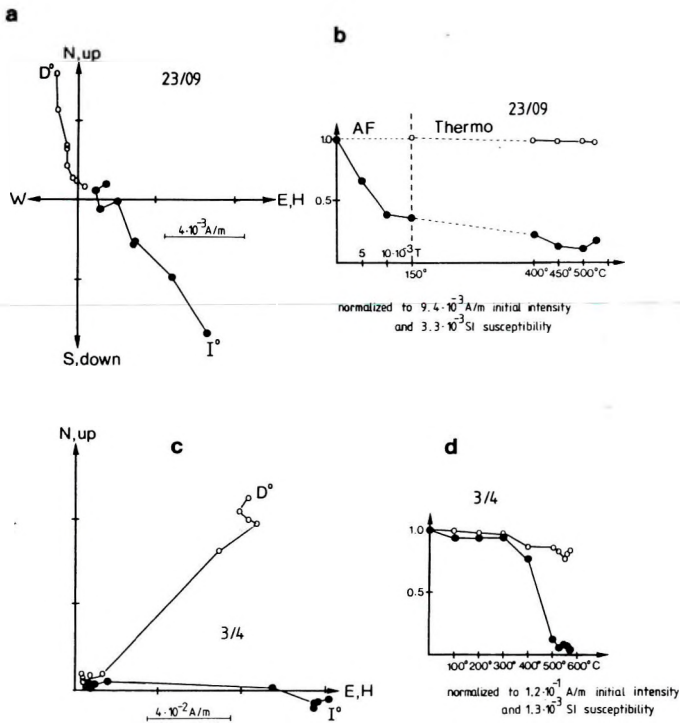


Fig. 4. Fast reduction of the NRM intensity on thermal demagnetization. a) and b): Wechsel unit, St. Corona, amphibolite (site 23); c) and d) Penninic, Markthodis, calcareous schist (site 3). For legend see Fig. 2

4. ábra. NRM gyors csökkenése hőkezelésre a) és b): Wechsel egység, St. Corona, amfibolit (23); c) és d) Penninikum, Markthodis, mészpala (3). Jelmagyarázat a 2. ábrán

Рис. 4. Быстрое убывание NRM при термической чистке. а) и б) Вехсельский покров, Ст. Корона, амфиболиты (23); в) и д) Пеннинский покров, Марктгодис, известковистые сланцы (3). Условные обозначения см. на рис. 2



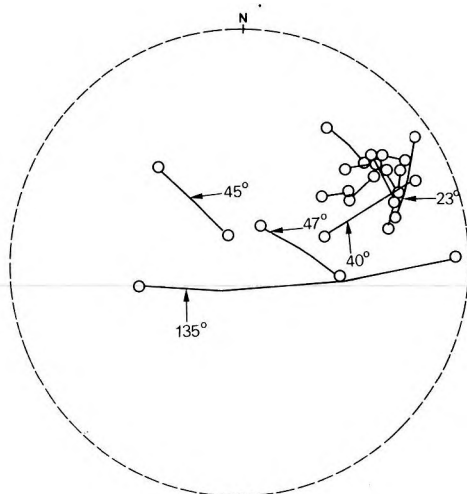


Fig. 5. Characteristic remanences for sister specimens. Wechsel unit, albite-chlorite schist (site 22). Stereographic projection, negative inclinations. ChRMs of sister specimens are joined and angular distances close to or higher than  $25^\circ$  marked

5. ábra. Ikerminták jellegzetes remanenciája. Wechsel egység, albit-klorit pala (22). Sztereografikus vetület, negatív inklinációk. Az ikerminták jellegzetes remanenciái össze vannak kötve és a  $25^\circ$ -nál nagyobb szögtávolságok megjelölve.

Рис. 5. Характерная остаточная намагниченность двойных проб. Вехсельский покров, альбит-хлоритовые сланцы (22). Стереографическая проекция, отрицательные наклонения. Значения характерной остаточной намагниченности соединены между собой с обозначением угловых расстояний свыше  $25^\circ$

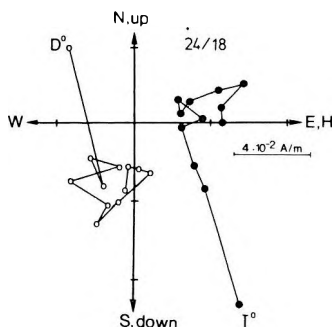


Fig. 6. Moderate instability of the NRM on thermal demagnetization. Penninic unit, Bernstein window, serpentinite (site 24)

6. ábra. Az NRM közepes instabilitása hőkezelésre. Penninikum, Bernstein ablak, serpentinit (24)

Рис. 6. Средняя нестабильность NRM при термической чистке. Пеннинский покров, Бернштайнское окно, серпентиниты (24)

Site	rock type	$n/n_0$	$D^*$ $D_c^*$	$I^*$ $I_c^*$	$k$	$\alpha_{95}$	cleaning
Rechnitz, Penninic, upper unit							
3	greenschist	5/11	43	-6	6	33.6	300° C
			53	+33	6	33.6	
4	greenschist	6/10	319	-57	4	40.8	300° C
			333	-34	4	40.8	
6	carbonatic schist	10/13	301	-37	11	15.2	150-300° C
			327	-25	11	15.2	
18	calcareous schist and phyllites	14/17	214	-29	18	9.6	300° C, 20-60 mT
			193	-35	18	9.6	
Rechnitz, Penninic, lower unit							
8	carbonatic schist	13/17	95	-2	5	19.6	300-400° C
			98	+8	5	19.6	
10	calcareous phyllite	12/25	113	-3	7	11.7	150-400° C
			115	+14	7	11.7	
Eisenberg, Penninic, lower unit							
12 <sub>1</sub>	greenschist	7/26	232	-23	18	14.4	250-350° C
			228	-23	18	14.4	
12 <sub>2</sub>	greenschist	17/26	286	-24	17	8.8	450-475° C
			283	-31	17	8.8	
14	greenschist	19/26	89	+2	4	18.9	150° C
			91	+20	4	18.9	
Palaeozoic of Graz							
13	greenschist	4/8	133	+47	84	10.0	50-150° C
			60	+64	84	10.0	
Bernstein, Penninic, upper unit							
24	serpentinite	19/19	287	+54	8	12.9	NRM
			-	-	-	-	
		14/19	139	-24	6	19.9	300-425° C
			-	-	-	-	
Wechsel unit							
22	albite-chlorite schist	9/13	58	-19	73	6.1	250-525° C
			56	+9	73	6.1	
Tertiary sediments							
19	Karthian sandstone	5/9	123	-36	11	23.9	300° C
			133	-54	11	23.9	
25	Badenian sediment	7/12	167	-42	7	25.0	20 mT
			165	-36	7	23.9	

Table 1. Palaeomagnetic data

$n$  – number of samples used for evaluation;  $n_0$  – number of collected samples;  $D^*$  – declination;  $I^*$  – inclination, before tectonic correction;  $D_c^*$ ,  $I_c^*$  – same after tectonic correction;  $k$  and  $\alpha_{95}$  – statistical parameters [FISHER 1953]

## I. táblázat. Paleomágneses adatok

$n$  – értelmezésbe bevont minták száma;  $n_0$  – begyűjtött minták száma;  $D^*$  – deklináció;  $I^*$  – inklináció tektonikai korrekció előtt;  $D_c^*$ ,  $I_c^*$  – ugyanaz tektonikai korrekció után;  $k$  és  $\alpha_{95}$  – statisztikai paraméterek [FISHER 1953]

## Таблица I. Палеомагнитные данные

$n$  – количество проб, использованных в интерпретации;  $n_0$  – количество отобранных проб;  $D^*$ ,  $I^*$  – склонение и наклонение до тектонической поправки;  $D_c^*$ ,  $I_c^*$  – то же с тектонической поправкой;  $k$  и  $\alpha_{95}$  – статистические параметры, по Фишеру (FISHER 1953)

7. ábra. Normalizált IRM felvétele: a)–d) és szuszceptibilitás-hőmérséklet görbék: e)–h).

Teli körök – normalizált intenzitás, üres körök – szuszceptibilitás

Рис. 7. Съемка нормированной IRM: а)–д) и кривые восприимчивость–температура е)–h).

Залитые кружки – нормированная интенсивность, полые кружки – восприимчивость





### 3. Magnetic mineralogy and susceptibility anisotropy

The vector plots indicate composite NRM in most cases. The magnetic minerals responsible for the different components of the NRM were not identified precisely. The behaviour of the NRM on cleaning, that of the susceptibility on heating, IRM experiments and the inspection of polished sections, however, permit one to make some conclusions about the magnetic minerals in the samples.

Normally the IRM curves show fast saturation (*Fig. 7/a, b, c*); the decay of the NRM on heating is also rapid while the susceptibility may increase (*Fig. 7/e*), decrease (*Fig. 7/f*) or remain constant (*Fig. 7/g*). Thus the magnetically soft mineral may be iron sulphide, as identified in the polished sections (sites

12 and 14) and/or maghemite (e.g. sites 3, 19). When the susceptibility remains stable, titanomagnetite is likely to carry the NRM (e.g. sites 18, 22, 24) since this mineral often occurs in the Penninic [KOLLER 1985].

In addition to a soft component, some specimens contain a phase which does not reach saturation in a field of 1.5 T. This is not likely to contribute to the NRM because the NRM versus temperature curve (*Fig. 7/h*) is similar to those with one soft component only.

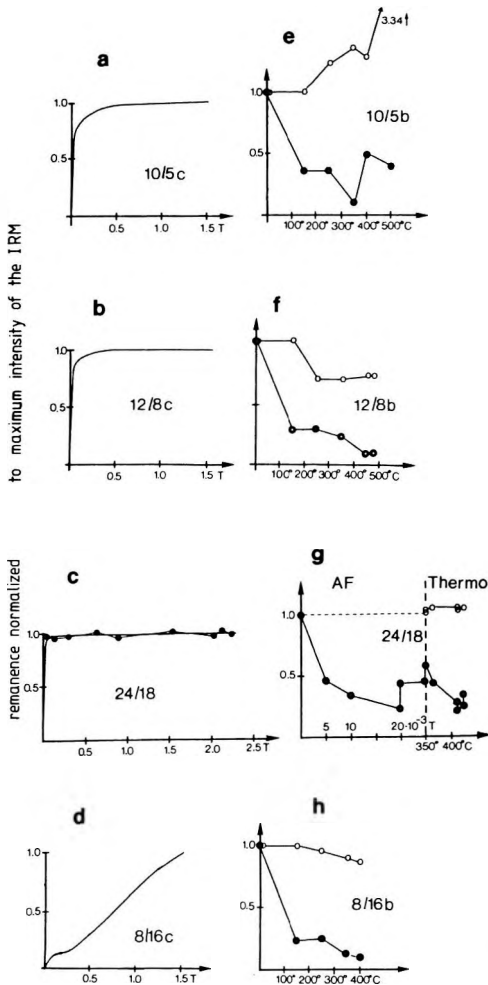


*Fig. 7.* Normalized IRM acquisition: a)–d) and susceptibility versus temperature curves: e)–h). Dots — normalized intensity, circles — susceptibility

Magnetic fabric was studied by measuring directional susceptibility in a low magnetic field. By analysing the magnitudes and orientations of the principal susceptibility axes and their relationship to the direction of the ChRM and the macroscopically observable schistosity planes we hoped to estimate the deflection of the directions of the ChRM of the ancient magnetic field due to anisotropy and the degree of complexity of the fabric.

Concerning the possible influence of magnetic anisotropy on the direction of the remanent magnetization, the observations can be summarized as follows. The degree of anisotropy is usually not high enough to cause considerable deflection from an external magnetic field due to magnetic anisotropy (*Table II*). Moreover, combined high and low field measurements indicate that the observed anisotropy is due largely to paramagnetic minerals (e.g. at site 12 entirely, at site 10, 90 per cent: ROCHETTE, personal communication).

The relationship between the orientation of the principal susceptibility axes and that of the fabric observable in the field is not straightforward. The directions of the principal susceptibility axes may be randomly distributed; if not, the minimum axes cluster, or define a great circle. In the last case, the great circle contains the pole of the macroscopically observable schistosity plane (*Figs. 8 and 9*). Such distribution may be explained by assuming that the minimum susceptibility directions, originally coinciding with the pole of the dominant schistosity, became displaced by adding a second 'component' to the original one during a later deformation process, or that the sampled rocks changed orientation in a constant stress field. The composite nature of the susceptibility is proved by the drastic reduction of the distance between extreme points along the great circle after heating, i.e. after having practically destroyed one of the magnetic minerals (*Fig. 9*).

A similar model may account for the fact that the statistically well-defined minimum susceptibility site mean directions often cluster away from the pole of the schistosity (*Fig. 10*). In this case, however, the deformation process responsible for the dominant fabric is totally overprinted.

Thus we may conclude that the magnetic fabric in itself or in relation to the texture of the studied metamorphics suggests that the rocks were subjected to complex tectonic and metamorphic processes. Our results, however, are indifferent to the timing, i.e. we cannot tell with any certainty whether the magnetic fabric was formed during one or during more metamorphic events.

In order to estimate the actual influence of the anisotropy on the direction of the remanence, remagnetization experiments were carried out. Some AF cleaned specimens were given IRM (*Fig. 11*) or ARM (*Fig. 12*), then stepwise heated and cooled in a laboratory field of controlled direction with the *X* (*Fig. 11*) or the *Z* (*Fig. 12*) axis parallel to the applied field. Remagnetization was complete or nearly complete at 435° C during a short heating run. The results of this experiment imply that

a) the directions of minimum susceptibility are close to the IRM directions (25/–3 and 349/–8) and the ARM directions (337/86, 340/57, 356/31, 180/31) respectively, i.e. the deflection from an external field due to the anisotropy of

Site	azimuth/dip		susceptibility anisotropy				ChRM $D^*/I'$
	b-axis	plane of schistosity	average	degree ( $k_{max}/k_{min}$ ) per cent max	min.	mean direction of min. (field system) azimuth/dip	
Rechnitz window, lower unit							
1	150/12	240/54	10	12	4	(120/54)	-
2	170/20	253/49	9	13	6	86/33	-
5	358/10	280/63	-	-	-	-	-
6	335/22	204/35	-	-	-	-	301/-37
7	160/18	135/15	-	-	-	-	-
10	340/3	260/20	5	8	1	*	(113/-3)
15	190/9	275/35	22	37	13	(67/6)	-
16	200/10	280/72	20	32	13	(143/55)	-
17x	10/10	320/40	20	25	13	160/61 97/60	-
Rechnitz window, upper unit							
3	205/29	187/31	38	72	4	108/71	(43/-6)
4	240/14	170/25	6	8	4	337/54	(319/-57)
8	310/18; 225/26	223/16	-	-	-	-	(95/-2)
9	60/10	125/16	-	-	-	-	-
11	230/10	260/13	-	-	-	-	-
18	358/17	282/41	9	28	3	*	214/-29
Eisenberg window, lower unit?							
12	275/95	320/9	6	8	4	*	286/-24 232/-23 (89/2)
14	-	245/20	-	-	-	-	-
Bernstein window, upper unit							
24	-	-	6	9	2	(39/71)	(287/54) (139/-24)
Graz Palaeozoic							
13	-	350/46	-	-	-	-	-
Wechsel unit							
21	50/25	50/30	-	-	-	-	-
22	220/20	248/28	12	16	7	94/62	58/-19
23	255/22	240/32	9	15	4	(185/47)	-
Karthian Sandstone covering Grogneiss unit							
19	-	10/20	3	9	1	(130/71)	123/-36

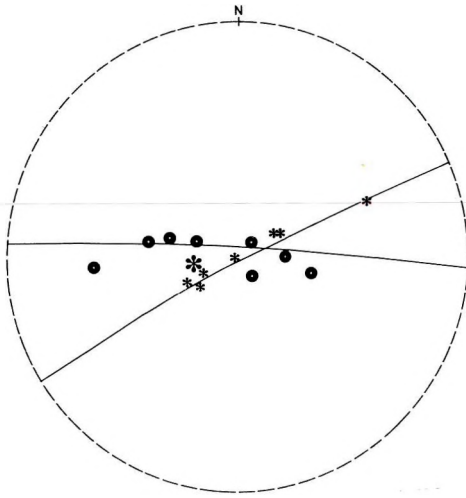
Table II. Oriented fabric: field observations and data from magnetic fabric analysis  
 Direction in brackets: poorly defined statistically ( $k < 10$  and/or  $\alpha_{95} > 15^\circ$ ); asterisk: minimum susceptibility directions define a great circle

II. táblázat. Irányított szövet: terepi megfigyelések és a mágneses szövetanalízis eredményei  
 Irányok zárójelben: statisztikailag gyengén meghatározott ( $k < 10$  és/vagy  $\alpha_{95} > 15^\circ$ );  
 csillag: minimum szuszceptibilitás irányok egy főkört határoznak meg

Таблица II. Ориентированная текстура на основании полевых наблюдений и магнитного текстурного анализа  
 Направления в скобке — статистически мало значимые ( $k < 10$  и/или  $\alpha_{95} > 15^\circ$ ); звезда — направлениями минимальной восприимчивости определяется дуга большой окружности

the susceptibility is indeed not significant;

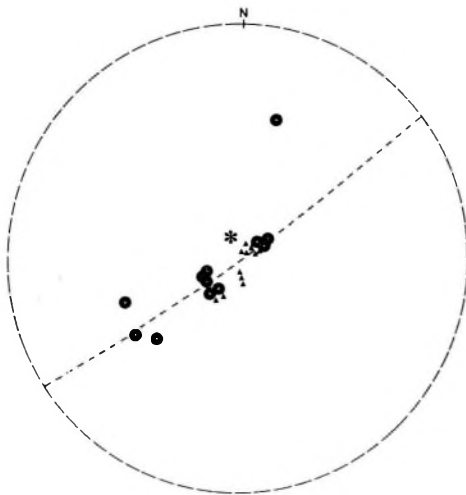
b) under geological conditions any previously existing NRM must have been totally overprinted during the last phase of metamorphism.



8. ábra. A minimum szuszceptibilitás irányok eloszlása egy főkörön (Hétforrásörs, mészfilit, 10). Sztereografikus vetület. Kör: a minimum szuszceptibilitás irányok gyűrődés nélküli rétegekben; kis csillag: palásság (és rétegződés) pólusa kismértékű gyűrődésekben; nagy csillag: ugyanez az általános palásságra.

Рис. 8. Распределение направлений минимальной восприимчивости вдоль дуги большой окружности (Хетфоррашёрш, известковистые филлиты, 10). Стереографическая проекция. Кружки — направления минимальной восприимчивости в нескладчатых прослоях; малые звезды — полюс сланцеватости (и слоистости) в небольших складках; крупные звезды — то же для общей сланцеватости

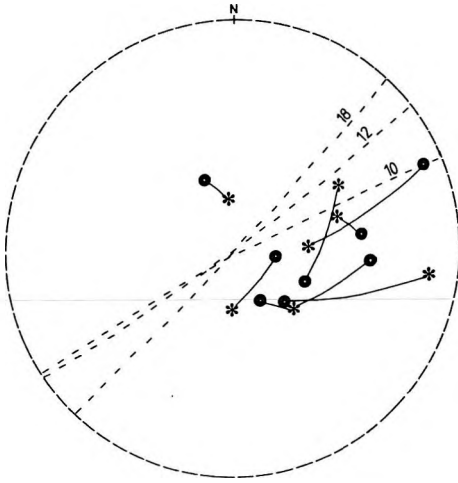
Fig. 8. Distribution of the directions of the minimum susceptibility along a great circle (Hétforrásörs, calcareous phyllite, site 10). Stereographic projection. Dots: directions of the minimum susceptibility in beds without small-scale folding; asterisks: poles of schistosity (and bedding) in small-scale folds (small asterisks) and that for the general schistosity (larger asterisk)



9. ábra. A minimum szuszceptibilitás irányok eloszlása egy főkörön (Felsőcsatár, zöldpala, 12). Sztereografikus vetület. Kör: a minimum szuszceptibilitás irányok a természetes állapotban; csillag: az általános palásság pólusa; háromszög: a minimum szuszceptibilitás irányok a minták 475° C-ra való hevítése, azaz a pirrhotit lebontása után

Рис. 9. Распределение направлений минимальной восприимчивости вдоль дуги большой окружности (Фельшечатар, зеленые сланцы). Стереографическая проекция. Кружки — направления минимальной восприимчивости в естественном состоянии; звезды — полюса общей сланцеватости; треугольники — направления минимальной восприимчивости после нагрева проб до 475°, то-есть после разложения пиррhotина

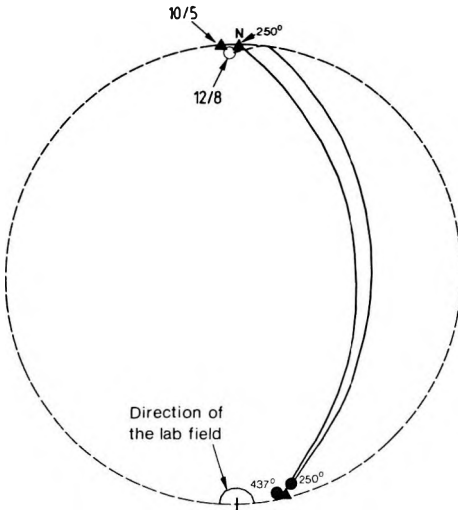
Fig. 9. Distribution of the directions of the minimum susceptibility along a great circle (Felsőcsatár, greenschist, site 12). Stereographic projection. Dots: directions of the minimum susceptibility in the natural state; asterisk: pole of the general schistosity; triangles: directions of the minimum susceptibility after heating the specimens at 475° C, i.e. destroying pyrrhotite



10. ábra. A palásság pólusának és a minimum szuszceptibilitás irányok összekötése a Penninikumra (1–11 és 15–17). Sztereografikus vetület, minden vektor lefelé mutat. A főkörök, amelyek mentén a minimumszuszceptibilitás irányok eloszlának (10, 12 és 18) szaggatott vonallal vannak jelölve.

Рис. 10. Соединение полюсов сланцеватости и направлений минимальной восприимчивости по Пеннинскому покрову (1–11 и 15–17). Стереографическая проекция. Все векторы направлены вниз. Дуги больших окружностей, вдоль которых распределены направления минимальной восприимчивости (10, 12 и 18), обозначены пунктирной линией

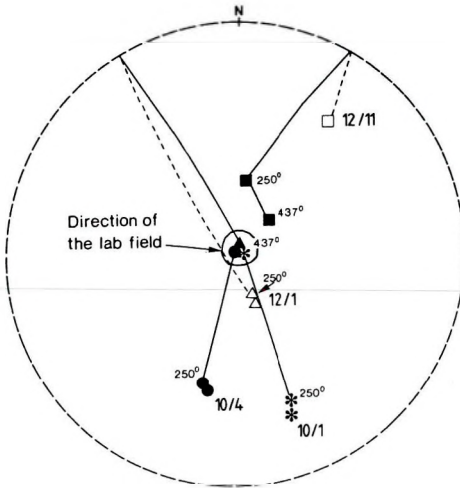
Fig. 10. Position of the pole of schistosity joined to the direction of minimum susceptibility(ies) for the Penninic unit (sites 1–4, 15–17). Stereographic projection, all vectors pointing downwards. The great circles along which the directions of minimum susceptibility are distributed at sites 10, 12, 18, respectively, are shown in dotted lines



11. ábra. A 10. és 12. mintavételi hely mintái IRM-jének újramágnesezése szabályozott laboratóriumi mágneses térben történő hevítéssel és hűtéssel. Sztereografikus vetület. Fekete jelek: lefelé mutató vektorok; üres jelek: felfelé mutató vektorok

Рис. 11. Перемагничивание IRM проб пунктов 10 и 12 при нагреве и остывании в регулируемом лабораторном магнитном поле. Стереографическая проекция. Жирные значки — векторы, направленные вниз; полые значки — векторы, направленные вверх

Fig. 11. Remagnetization of IRM of samples from sites 10 and 12 by heating and cooling them in a controlled laboratory field. Stereographic projection. Solid symbols: vectors pointing downwards; hollow symbols: vectors pointing upwards



12. ábra. A 10. és 12. mintavételi hely mintái ARM-jének újramágnesezése szabályozott laboratóriumi mágneses térben történő hevítéssel és hűtéssel. Sztereografikus vetület. Fekete jelek: lefelé mutató vektorok, üres jelek: felfelé mutató vektorok

Рис. 12. Пермагничивание ARM проб пунктов 10 и 12 при нагреве и остывании в регулируемом лабораторном магнитном поле. Стереграфическая проекция. Жирные значки — векторы, направленные вниз; полые значки — векторы, направленные вверх

Fig. 12. Remagnetization of ARM of samples from sites 10 and 12 by heating and cooling in a controlled laboratory field. Stereographic projection. Solid symbols: vectors pointing downwards; hollow symbols: vector pointing upwards

#### 4. Tectonic implication

Due to high between-site scatter for all the studied units — both before and after tectonic correction — precise palaeomagnetic directions cannot be defined for any of the units. Nevertheless, certain rotation trends can be recognized.

The main problem in interpretation is caused by the spread in inclination (Fig. 13). It may be argued that a metamorphic rock at the time of acquisition of the ChRM might have been oriented differently from both the present and the tectonically corrected position.

It stands to reason, however, that the position at the critical time interval be assumed as constrained by the present horizontal on the one hand, and by the plane of schistosity (stratification) observed in the field, on the other. As Table I shows, the tectonic correction has but little effect on the direction of the ChRM. Thus the low inclinations are difficult to account for, once the mid-Tertiary age of the last metamorphic event is accepted, and the composite or deflected nature of the ChRM is ruled out. In fact, some of the inclinations are so shallow, both before and after tectonic correction, that they are indicative of a pre-Tertiary, probably Palaeozoic magnetization (sites 8, 10, 14). It is interesting to note, therefore, that previously Palaeozoic was the age assigned to the Rechnitz and Eisenberg windows [FÖLDEVÁRI et al. 1948, SZEBÉNYI 1948].

Apart from sites 8, 10, and 14, the Rechnitz window is characterized by large to moderate clockwise declination rotations. Sites 3 (fully or partly corrected for tectonic position), 18, and 12<sub>1</sub> form a moderately rotated group together with 13 (Graz Palaeozoic, corrected), while 6 and 12<sub>2</sub> show excess

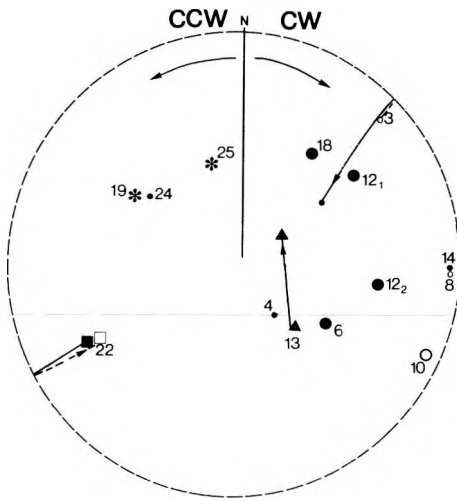


Fig. 13. Palaeomagnetic inclinations before tectonic correction in the eastern part of the Eastern Alps. Stereographic projection. Full symbols: positive inclination; hollow symbols: negative inclination. Circles are for the Penninic unit, triangle for the Palaeozoic of Graz, square for the Wechsel unit, asterisks for Tertiary sediments. Small symbols:  $\alpha_{95} > 15^\circ$ , larger symbols:  $\alpha_{95} \leq 15^\circ$

13. ábra. Paleomágneses inklinációk tektonikai korrekció előtt a Keleti Alpok keleti részében. Sztereografikus vetület. Fekete jelek: pozitív inklináció, üres jelek: negatív inklináció. Kör: Penninikum, háromszög: grazi paleozoikum, négyzet: Wechsel egység, csillag: harmadkori üledék. Kis jelek:  $\alpha_{95} > 15^\circ$ , nagy jelek:  $\alpha_{95} \leq 15^\circ$

Рис. 13. Палеомагнитные наклонения до тектонических поправок на восточном окончании Восточных Альп. Стереографическая проекция. Жирные значки — положительные наклонения; полые значки — отрицательные наклонения. Кружки — Пеннинский покров, треугольник — грацкий палеозой, квадрат — Вехсельский покров, звезды — третичные отложения. Малые значки —  $\alpha_{95} > 15^\circ$ , крупные значки —  $\alpha_{95} \leq 15^\circ$

rotation. The declination at sites 8, 10, 14 also deviate by a large angle from the north which may be interpreted as clockwise rotation. It is possible that on the CW side of Fig. 13 we see an older magnetization with more and a younger one with less declination rotation, since at site 12 the component with higher unblocking temperature ( $12_2$ ) shows large deviation, the less resistant one ( $12_1$ ) only moderate deviation from the present north.

The rotation angle for a single site from the Wechsel unit (Fig. 13, 22) is high, though the sense of rotation is undecided.

A single site from the highest level of the Rechnitz unit (24), and Tertiary sediments (sites 19, 25) covering the Grobgness unit (which is in turn underlain by the Wechsel) show counterclockwise rotation. The similarity of the directions observed for sites 24 and 19 implies Miocene rotation for the first of these.

The timing of the rotations observed for the rest of the metamorphics is less straightforward. Some of the ChRMs may predate the Miocene metamorphism (e.g. sites 8, 10, 14). This idea is supported, for instance, by observations on the metamorphic texture in the Eisenberg window by LELKES-FELVÁRI (personal communication) who suggests that the high-pressure low-temperature Eo-Alpine metamorphism was not everywhere overprinted by a younger greenschist facies metamorphism. Even if some of the ChRMs are older, there are others which are of Miocene age, implying that significant clockwise rotations took place between 20 Ma and the magnetization of the Styrian volcanics — that show no rotation [MAURITSCH and BECKE 1987]. The young age of the rotations in the Rechnitz area is supported in an indirect way by the orientation of the magnetic fabric.



As we have already noted the pole of the plane of schistosity (oriented by the strongest metamorphism) and the directions of the minimum susceptibilities (oriented by the last metamorphism) for the same site define a great circle. These great circles always deviate from north–south orientation (Fig. 10). When corrected for the measured palaeomagnetic rotations, these great circles become N–S oriented, thus reflecting a stress field which is expected in the Neogene as a consequence of the collision between stable Europe and the African plate.

### Acknowledgement

We are grateful to P. Rochette for the high-field anisotropy measurements and evaluation. We thank R. Bordás for assistance with the low-field anisotropy measurements and F. Heller for the critical reading of the manuscript.

### REFERENCES

- FISHER R. A. 1953: Dispersion on a sphere. *Proc. Roy. Soc. Lond. A.*, **217**, pp. 295–305
- FÖLDVÁRI A., NOSZKY J., SZEBÉNYI L. and SZENTES F. 1948: Geological observations in the Kőszeg area (in Hungarian). Report of the Hungarian Finance Ministry, 1947–1948, pp. 5–31
- GRATZER R. 1985: Vergleichende Untersuchungen an Metabasiten im Raum Hannersdorf, Burgenland. Aus den Sitzungsberichten der ÖAW, Mathematisch–Naturwissenschaftliche Klasse, Abt. I, **194**, 6–10, pp. 132–148, Wien
- KOLLER F. 1985: Petrologie und Geochemie der Ophiolite des Penninikums am Alpenostrand. *Jahrbuch d. Geol. Bundesanstalt* **128**, 1, pp. 83–150, Wien
- LELKES-FELVÁRI Gy. 1982: A contribution to the knowledge of the Alpine metamorphism in the Kőszeg–Vashegy area. *Neues Jb. Geol. Palaont. Monatshefte* **5**, pp. 297–305
- MAURITSCH H. J. and BECKE M. 1987: Paleomagnetic Investigations in the Eastern Alps and the Southern Border Zone. In *Geodynamics of the Eastern Alps*, Flügel H. W. and Faupl P. (eds), pp. 282–308 Deuticke, Vienna
- PAHR A. 1980: Die Fenster von Rechnitz, Bernstein, und Möltern. in OBERHAUSER R.: *Der Geologische Aufbau Österreichs*, pp. 320–326, Wien
- SCHMIDT W. J. 1951: Überblick über geologische Arbeiten in Österreich. *Zeitschrift d. Deutschen Geol. Gesellschaft* **102**, Hannover, pp. 311–316
- SCHÖNLAUB H. P. 1973: Schwamm–Spiculae aus dem Rechnitzer Schiefergebirge und ihr stratigraphischer Wert. *Jahrbuch d. Geol. Bundesanstalt* **116**, pp. 35–49, Wien
- SZEBÉNYI L. 1948: Geology of the Hungarian part of the Eisenberg (in Hungarian). Report of the Hungarian Finance Ministry, 1947–1948, pp. 45–50

## ERŐSEN METAMORFIZÁLT KŐZETEK PALEOMÁGNESES VIZSGÁLATA: KELETI ALPOK (AUSZTRIA ÉS MAGYARORSZÁG)

Herman J. MAURITSCH, MÁRTONNÉ SZALAY Emő és Alfred PAHR

Tektonikailag bonyolult terület paleomágneses vizsgálatát végeztük elsősorban erősen metamorfizált kőzetek mintázásával. Kilenc mintavételi hely esett a Penninikumra, egy a grazi paleozoikumra és egy a Wechsel egységre. Mindezek jellegzetes remanens mágnesezettséget adtak, amelyet tovább ellenőriztünk a metamorfózis okozta lehetséges torzítás korának és nagyságának felbecslésével. Arra az eredményre jutottunk, hogy a tanulmányozott metamorf kőzetek teljesen átmágneseződtek a metamorfózis utolsó szakaszában és az orientált mágneses szövetnek csak elhanyagolható hatása lehetett a remanens mágnesezettség irányára.

A jellegzetes remanencia-irányok — mind tektonikai korrekció előtt, mind után — határozottan eltérnek a terület jelenlegi mágneses terétől. A szórás túl nagy, így egyetlen tektonikai egységre sem tudtunk paleomágneses irányokat definiálni. Ennek ellenére a deklináció-rotációk tendenciái felismerhetők és mint tektonikai rotációk értelmezhetők. A Penninikum óramutató járásával meg egyező, a Penninikum teteje viszont — a kárpáti és bádeni fedővel együtt — óramutató járásával ellentétes rotációt szenvedett. A Wechsel egység rotációja bizonytalan az igen lapos inklinációk miatt. A megfigyelt rotációk elsősorban középső-miocén tektonikai mozgásokhoz köthetők, amelyek mind a kárpáti üledék, mind a metamorfózis legutolsó fázisa (20 Ma) koránál fiatalabbak.

## ПАЛЕОМАГНИТНОЕ ИЗУЧЕНИЕ СИЛЬНО МЕТАМОРФИЗОВАННЫХ ПОРОД: ВОСТОЧНЫЕ АЛЬПЫ (АВСТРИЯ И ВЕНГРИЯ)

Герман И. МАУРИЧ, Змё МАРТОН-САЛАИ, Альфред ПАР

Было проведено палеомагнитное изучение района со сложным тектоническим строением путем опробования в первую очередь сильно метаморфизованных пород. Девять пунктов пробоотбора были в пределах Пеннинского покрова, один — грацкого палеозоя, и один — Вехсельского покрова. Во всех обнаружена характерная остаточная намагниченность, которая была проверена путем оценки возраста и масштаба искажений, возможных вследствие метаморфизма. Был сделан вывод о том, что изученные метаморфические породы были целиком перемагничены в последнюю стадию метаморфизма и что ориентированная магнитная структура могла оказать лишь пренебрегаемое влияние на направление остаточной намагниченности.

Характерные направления остаточной намагниченности — как до, так и после тектонической поправки — существенно отличаются от современного магнитного поля региона. Разброс значений слишком велик, так что палеомагнитные направления не могли быть определены для каждой тектонической единицы в отдельности. Несмотря на это, тенденции к повороту склонений могут быть установлены и интерпретированы в качестве тектонических. Пеннинский покров обнаруживает поворот по часовой стрелке, а его верхи — совместно с карпатским и баденским чехлом — против часовой стрелки. Поворот Вехсельского покрова устанавливается ненадежно в связи с малыми наклонениями. Наблюдаемые повороты могут быть связаны в первую очередь со среднемиоценовыми тектоническими движениями, проявившимися как после накопления карпатских отложений, так и после последней фазы метаморфизма (20 млн. лет).

